

# Multi-component force sensor based on multiplexed fibre Bragg grating strain sensors

A Fernandez Fernandez<sup>1,2</sup>, F Berghmans<sup>1,3</sup>, B Brichard<sup>1</sup>,  
P Mégret<sup>4</sup>, M Decréton<sup>1,2</sup>, M Blondel<sup>4</sup> and A Delchambre<sup>2</sup>

<sup>1</sup> SCK-CEN, Belgian Nuclear Research Centre, Instrumentation Department, Boeretang 200, B-2400 Mol, Belgium

<sup>2</sup> Université libre de Bruxelles, CP165/41, 50 avenue F D Roosevelt, B-1050 Brussel, Belgium

<sup>3</sup> Vrije Universiteit Brussel, Pleinlaan 2, B-1050, Brussel, Belgium

<sup>4</sup> Faculté Polytechnique de Mons, 31 Boulevard Dolez, B-7000 Mons, Belgium

E-mail: afermand@sckcen.be

Received 10 January 2001, accepted for publication 22 March 2001

## Abstract

The control of robots in electromagnetically noisy environments may benefit from the use of EMI-insensitive multi-component force sensors.

Multi-component force sensing is usually done with local strain measurements on an elastic transducer. We propose to use fibre Bragg grating (FBG) strain sensors to perform these local strain measurements, taking advantage of their multiplexing capabilities and their immunity to electromagnetic interference. In this paper, we discuss the design and the calibration of a compact multi-component force sensor using an elastic transducing body and eight multiplexed fibre Bragg gratings.

We demonstrate, for the first time, that multi-component force sensors based on multiplexed FBG strain sensors can be constructed.

**Keywords:** force, torque, strain, fibre optic sensor, fibre Bragg gratings, Maltese-shape transducer, robotics, robot feedback control

(Some figures in this article are in colour only in the electronic version; see [www.iop.org](http://www.iop.org))

## 1. Introduction

The use of robots and manipulators in complex applications such as assembly, surface machining and cutting operations requires efficient multi-component force sensing schemes to control the force exerted by the robot end-effector on an object. Since such remote-handled tools also have to operate in electromagnetically noisy environments, classical force sensors based on electrical strain gauges require a complex design and need a large number of shielded connections.

To tackle this problem, we rely on passive fibre Bragg grating (FBG) strain sensors [1–3]. Their multiplexing capabilities allow us to construct very compact sensors, with a reduced number of connections to the instrumentation. In this paper, we demonstrate that it is possible to perform a multi-component force measurement by means of multiplexed FBG strain sensors mounted on a force uncoupling elastic body.

## 2. Multi-component force sensor based on FBG strain sensors

Generally, a classical force sensor is a structure with a dedicated shape to uncouple the different components of the applied force [4–10]. The forces and moments applied to the sensor are evaluated through  $n$  strain measurements, performed by appropriate strain transducers, at given locations on the sensor body. The force vector components are derived from these strain measurements, yielding an output vector  $z = [z_1 z_2 \dots z_n]^T$ .

If the sensor body has been designed to remain in the elastic region, the superposition principle applies. The relationship between internal strains and external forces is therefore linear. This can be written in a matrix form:  $[z_1 z_2 \dots z_n]^T = C[F_x F_y F_z M_x M_y M_z]^T$ , where  $C$  is a  $n \times 6$  matrix called the *calibration matrix*. This relation needs to be

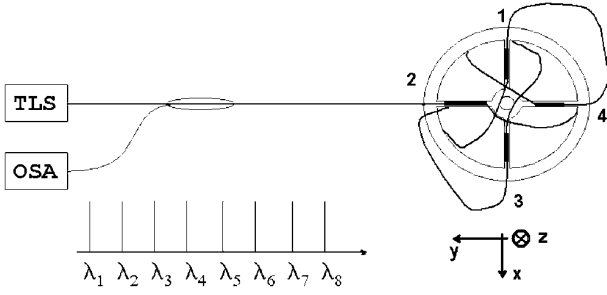


**Figure 1.** Schematic view of the multi-component force sensor based on eight multiplexed FBG strain sensors. We number the beams counterclockwise.

inverted to derive the force components from the measurement of  $n$  strain transducers. When the number of strain transducers is not equal to six, pseudo-inverse matrix calculations have to be used [7, 11].

As proof-of-principle for multi-component force sensing with FBG sensors, we started from the most widespread multi-component force sensor design: the Maltese-cross-shaped transducer [12]. We constructed a three-component force sensor ( $F_z, M_x, M_y$ ) with eight multiplexed FBG sensors glued in the centre of the beams (cf figure 1). Our force sensor design consists of four radial beams of 50 mm length that connect a rigid hub of 25 mm radius to an outer flange. The beams have a square cross-subsection of 4 mm  $\times$  4 mm. The elastic body is made of a high-yieldpoint stainless steel. Eight fibre Bragg gratings, spaced by 4 nm in the window 1525–1560 nm, were bonded to the sensor body using Loctite cyanoacrylate adhesive 401. To compensate for the possible temperature effects and the drift of the wavelength detection scheme, two FBG strain sensors, with successive Bragg wavelengths, were mounted on the opposite faces of the beam. The temperature is assumed to be uniform on the whole sensor. The strain on beam  $i$  is therefore measured by subtracting two respective Bragg peak shifts, resulting in a compensated wavelength shift  $\Delta\lambda_i$  [13].  $F_z, M_x$  and  $M_y$  can therefore be computed by inverting  $[\Delta\lambda_1 \Delta\lambda_2 \Delta\lambda_3 \Delta\lambda_4]^T = C[F_z M_x M_y]^T$ .

Due to the symmetry of the elastic transducer, the theoretical form of the calibration matrix  $C$  is given by

$$\begin{pmatrix} \Delta\lambda_1 \\ \Delta\lambda_2 \\ \Delta\lambda_3 \\ \Delta\lambda_4 \end{pmatrix} = \begin{pmatrix} a & -b & 0 \\ a & 0 & -b \\ a & b & 0 \\ a & 0 & b \end{pmatrix} \begin{pmatrix} F_z \\ M_x \\ M_y \end{pmatrix}. \quad (1)$$

Multi-component force sensors are commonly evaluated using the method proposed by Uchiyama and Bayo, based on the singular value decomposition of the normalized calibration matrix [14–17]. Uchiyama *et al* [14] established that the relative error on the determination of the force components  $\|\Delta\mathbf{f}\|/\|\mathbf{f}\|$  is related to the relative error on the strain measurements  $\|\Delta\lambda\|/\|\lambda\|$  by the following relation:

$$0 \leq \frac{\|\Delta\mathbf{f}\|/\|\mathbf{f}\|}{\|\Delta\lambda\|/\|\lambda\|} \leq \frac{\sigma_1(C_{norm})}{\sigma_6(C_{norm})} \quad (2)$$

where  $\sigma_1(C_{norm})$  and  $\sigma_6(C_{norm})$  are the largest and the smallest singular values of  $C_{norm}$ <sup>5</sup>. The ratio  $\sigma_1(C_{norm})/\sigma_6(C_{norm})$

<sup>5</sup> The definition of the singular value decomposition of matrices can be found in [18].

represents the condition number of the multi-component force sensor. The condition number sets an upper bound to the relative error propagation between measured strains and forces. A condition number of one represents the lowest possible error propagation. A complete discussion on error propagation has been provided by Bicchi and Canepa [19].

### 3. Experimental results

We calibrated the force sensor by applying pure forces  $F_z$  and pure torques  $M_x$  and  $M_y$  by means of well defined weights and a system of pulleys (see figure 3).

We evaluated the calibration matrix  $C$  following the standard calibration procedure described by Watson and Drake [7] and by Shimano and Roth [8]. The calibration range was from 0 N to 475 N for  $F_z$  and 0 N m until 6.5 N m for both torques. The temperature fluctuations during the calibration did not exceed 0.5 °C. The results are summarized in figure 2, which also shows the spectra reflected by these FBGs, as measured with an ANRITSU MS9710C optical spectrum analyser (OSA) and a ANRITSU MG9637A tunable laser source (TLS), with a 17.5 pm step.

For the calibration matrix  $C$ , with the force  $F_z$  expressed in N and the torques  $M_x, M_y$  in N m, we find

$$\begin{pmatrix} \Delta\lambda_1 \\ \Delta\lambda_2 \\ \Delta\lambda_3 \\ \Delta\lambda_4 \end{pmatrix} = \begin{pmatrix} 0.32 & -54.0 & -2.5 \\ 0.03 & 1.6 & -40.7 \\ 0.35 & 61.0 & -0.9 \\ 0.85 & 2.5 & 66.8 \end{pmatrix} \begin{pmatrix} F_z \\ M_x \\ M_y \end{pmatrix}. \quad (3)$$

The experimental calibration matrix (3) needs to be inverted to derive the force components from the measurement of the FBG strain sensors. We calculated the inverse relation by using the Moore–Penrose inversion [11], after normalizing with respect to the maximum forces and torques [14, 15]. We obtain therefore the normalized calibration matrix  $C_{norm}$

$$\begin{pmatrix} F_z \\ M_x \\ M_y \end{pmatrix} = (C_{norm}^T C_{norm})^{-1} C_{norm}^T \begin{pmatrix} \Delta\lambda_1 \\ \Delta\lambda_2 \\ \Delta\lambda_3 \\ \Delta\lambda_4 \end{pmatrix} \quad (4)$$

$$= \begin{pmatrix} 391.149 & 401.436 & 324.930 & 263.604 \\ -0.057 & -0.001 & 0.057 & -0.002 \\ -0.049 & -0.092 & -0.042 & 0.039 \end{pmatrix} \begin{pmatrix} \Delta\lambda_1 \\ \Delta\lambda_2 \\ \Delta\lambda_3 \\ \Delta\lambda_4 \end{pmatrix} \quad (5)$$

### 4. Discussion

A comparison of the experimental calibration matrix (3) with the theoretical form (1) shows that the force sensor operates well for both torque components. A good discrimination between force components is achieved. The  $M_x$  and  $M_y$  calibrations evidence the linear response of the force sensor as well as its ability to separate the desired force component from all the others. Nevertheless, the  $F_z$  calibration does not give the expected results. The measurement of the  $F_z$  component is only achieved satisfactorily by two pairs of FBGs. This is probably due to a non-uniformity in the gluing conditions for the different FBG pairs.

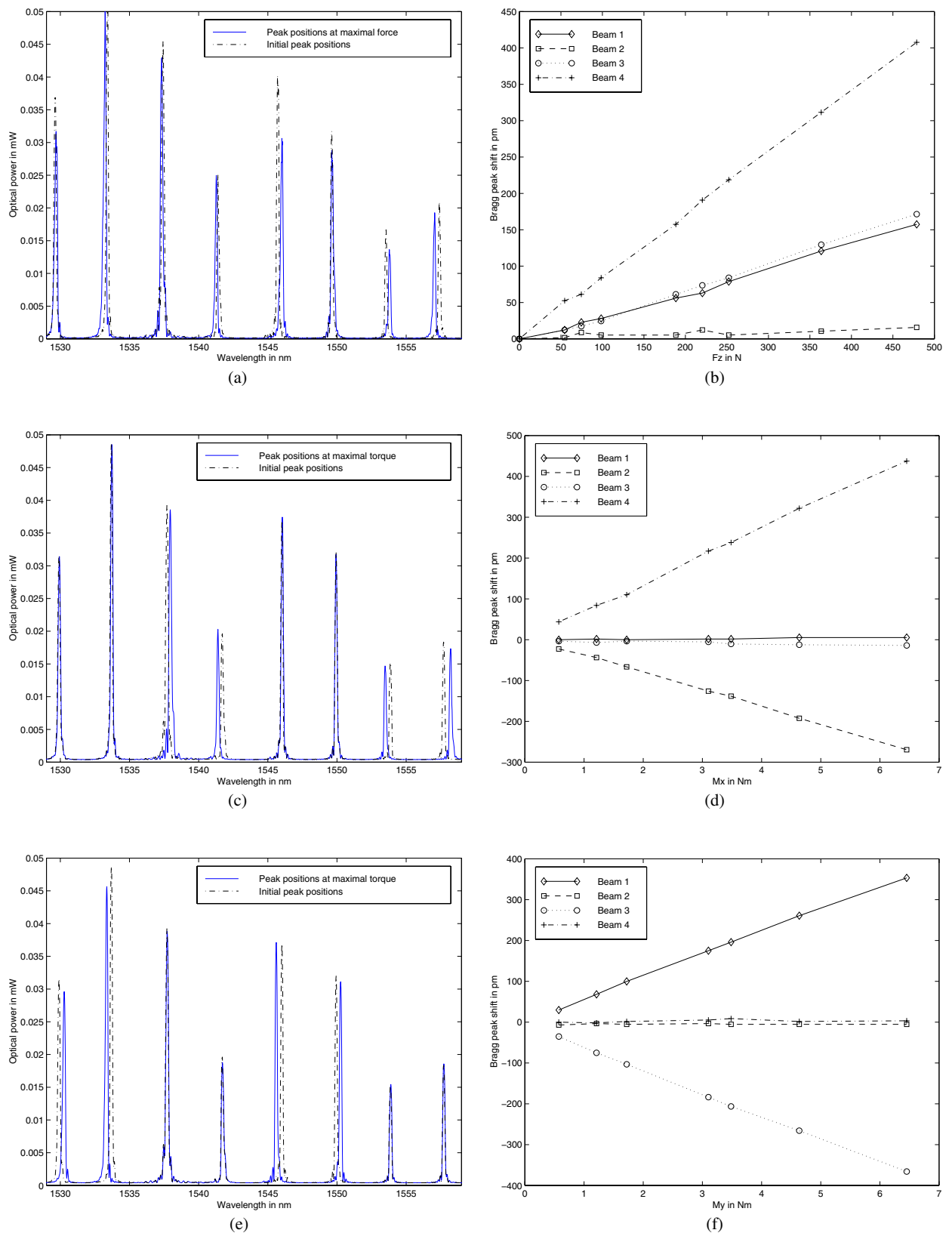


**Figure 2.** Calibration results of our multi-component force sensor based on multiplexed FBG strain sensors. (a) Bragg peak shifts during the  $F_z$  calibration. The four beams should be equally stressed. (b)  $F_z$  calibration. (c) Bragg peak shifts during the  $M_x$  calibration. Beam 2 and beam 4 show opposite strains while beam 1 and beam 3 are not stressed. (d)  $M_x$  calibration. (e) Bragg peak shifts during the  $M_y$  calibration. Beam 1 and beam 3 show opposite strains while beam 2 and beam 4 are not stressed. (f)  $M_y$  calibration.



**Figure 3.** The calibration table allowing forces and torques to be applied. On the right, we see the single fibre connecting the sensor with its instrumentation.

The singular values of the FBG multi-component sensor are {12.596, 11.985, 0.001} (cf equation (2)). These values confirm the correct operation of the sensor with respect to the torque component measurements, while they evidence the force component measurement limitation. Our future work will therefore focus on the improvement of the  $F_z$  measurement by optimizing both the mounting of the FBG strain sensors and their position on the elastic transducer. A possible solution could be to attach prestressed FBGs only at two points and allow operation in both tensile and compressive mode. With this configuration, the requested torque measurement requires a new transducer design that transforms torques in compression or tension, as has been done in multi-component force sensors based on LVDT extensometers [20].

## 5. Conclusions

Robot operation in complex manufacturing tasks requires efficient multi-component force sensors. FBG sensing technology could allow us to develop compact force sensors able to operate in harsh environments. For the first time, we demonstrate that multi-component force sensors based on multiplexed FBG strain sensors can be constructed. A design based on a Maltese-cross-shaped elastic transducer has been evaluated and its satisfactory operation has been evidenced.

Nevertheless, in this application, the control of the gluing conditions is a critical issue. Future work will therefore focus on the study of the repeatability of the gluing procedure for FBGs intended for multi-component force sensing. It will also include the evaluation of the actual efficiency of the temperature compensation. FBGs written in polarization-maintaining fibres [21] as intrinsic multi-component force transducers will also be investigated.

## References

- [1] Othonos A and Kalli K 1999 *Fiber Bragg Gratings: Fundamentals and Applications in Telecommunications and Sensing* (Artech House Optoelectronics Library) (Boston, MA: Artech House Publishers)
- [2] Rao Yun-Jiang 1997 In-fibre Bragg grating sensors *Meas. Sci. Technol.* **8** 355–75
- [3] Grattan K T V and Meggit B T 1998 *Optical Fiber Sensor Technology* vol 2 (London: Chapman and Hall)
- [4] Flatau C R 1976 Force sensing in robots and manipulators *Proc. 2nd Int. CISM IFT.MM Symp. on the Theory and Practice of Robots and Manipulators* pp 294–306
- [5] Hirose S and Yoneda K 1990 Development of optical 6-axial force sensor and its signal calibration considering non linear calibration *Proc. Int. Conf. on Robotics and Automation* pp 46–53
- [6] Scheinman V 1969 Design of a computer controlled manipulator *MS Thesis* Stanford University, Mechanical Engineering Department
- [7] Watson P C and Drake S H 1977 Pedestal and wrist force sensors for automatic assembly *Proc. 5th Int. Symp. on Industrial Robots* pp 501–11
- [8] Shimano B and Roth B 1977 On force sensing information and its use in controlling manipulators *Proc. IFAC Int. Symp. on Information-Control Problems* pp 119–26
- [9] Van Brussel H, Belien H and Thielemans H 1986 Force sensing for advanced robot control *Robotics* **2** 138–48
- [10] Rosen C A and Nitzan D 1997 Use of sensors in programmable automation *Computer* **10** 12–23
- [11] Klema V C and Laub A J 1980 The singular value decomposition: its computation and some applications *IEEE Trans. Automat. Control* **25** 164–76
- [12] Gorinevsky D M, Formalsky A M and Schneider A Y 1997 *Force Control of Robotics Systems* (New York: Chemical Rubber Company)
- [13] Xu M G, Archambault J L, Reekie J L and Dakin J P 1997 Thermally-compensated bending gauge using surface-mounted fibre gratings *Int. J. Optoelectron.* **9** 281–3
- [14] Uchiyama M, Bayo E and Palma-Villalon E 1991 A systematic design procedure to minimize a performance index for robot force sensors *J. Dyn. Syst. Meas. Control* **113** 388–94
- [15] Bicchi A 1990 *A Criterion for the Optimal Design of Multi-axis Force Sensors* (Cambridge, MA: MIT Press)
- [16] Bayo E and Stubbe S R 1989 Six axis force sensor evaluation and a new type of optimal frame/truss design for robotics applications *J. Robot. Syst.* **6** 191–208
- [17] Uchiyama M, Nakamura Y and Hakamori K 1991 Evaluation of the force robot structure using singular value decomposition *Adv. Robot.* **5** 39–52
- [18] Trefethen L N and Bau D 1997 *Numerical Linear Algebra* (Philadelphia: SIAM)
- [19] Bicchi A and Canepa G 1994 Optimal design of multivariate sensors *Meas. Sci. Technol.* **5** 319–32
- [20] Piller G 1986 A compact six-degree-of-freedom force/torque sensor for assembly robots *Tactile and Non-Vision (Robot Sensors 2)* ed A Pugh (IFS) pp 66–74
- [21] Udd E, Lawrence C M and Nelson D V 1997 Multiple axis strain sensing using fiber Bragg gratings written onto birefringent single mode optical fiber *Proc. 12th Int. Conf. on Optical Fiber Sensors* vol 16, pp 48–51